Predicting Device-to-Device Channels From Cellular Channel Measurements: A Learning Approach

Mehyar Najla, *Student Member, IEEE*, Zdenek Becvar, *Senior Member, IEEE*, Pavel Mach, *Member, IEEE*, and David Gesbert, *Fellow, IEEE*

***Abstract*— Device-to-device (D2D) communication, which enables a direct connection between users while bypassing the cellular channels to base stations (BSs), is a promising way to offload the traffic from conventional cellular networks. In D2D communication, optimizing the resource allocation requires the knowledge of D2D channel gains. However, such knowledge is hard to obtain at reasonable signaling costs. In this paper, we show this problem can be circumvented by tapping into the information provided by the estimated cellular channels between the users and surrounding BSs as these channels are estimated anyway for a normal operation of the network. While the cellular and D2D channel gains exhibit independent fast fading behavior, we show that average gains of the cellular and D2D channels share a non-explicit relation, which is rooted into the network topology, terrain, and buildings setup. We propose a deep learning approach to predict the D2D channel gains from seemingly independent cellular channels. Our results show a high degree of convergence between the true and predicted D2D channel gains. Moreover, we demonstrate the robustness of the proposed scheme against environment changes and inaccuracies during the offline training. The predicted gains allow to reach a near-optimal capacity in many radio resource management algorithms.**

***Index Terms*— Device-to-device, channel prediction, deep neural networks, supervised machine learning.**

I. Introduction

IN DEVICE-TO-DEVICE (D2D) communication, data is transmitted over a direct link between a pair of nearby user equipment (UEs) instead of being relayed via a base station (BS) [1], [2]. Conventionally, the D2D pairs can exploit two communication modes: shared and dedicated [3]. In the shared mode, the D2D pairs reuse the same radio resources as cellular users (CUEs) that send data through the BS [4]. On the contrary, the D2D pairs in the dedicated mode are allocated with resources that are orthogonal to the resources of CUEs [5].

An efficient exploitation of the D2D network often entails challenging radio resource management (RRM) problems, such as, selection between shared and dedicated modes [5]–[9], interference management to/from CUEs [10]–[13], channels and power allocation [14]–[21], to name a few. Conventional algorithms addressing the above RRM problems in D2D networks assume a prior estimation of the D2D channel gains (i.e., channel gains among all UEs involved in D2D). In some cases, the full knowledge can be relaxed to a partial knowledge, where only a subset of the distributed D2D channel gains is required (e.g., in [19]). Nevertheless, even the partial knowledge of the D2D channel gains implies a substantial cost in terms of an additional signaling overhead on top of the one generated in classical cellular communications. In fact, the cellular channel gains (i.e., channel gains between the UEs and the BSs) are typically estimated by default as these are needed for handover as well as user attachment, authorization, and classical cellular communication purposes. More precisely, even the users that wish to engage in D2D communications must be recognized by the network and thereby their cellular channel gains must be estimated initially. Thus, these cellular channels are periodically reported to the BSs, and can be leveraged at no additional signaling overhead. An interesting question then arises as to whether the by-default cellular channel gains carry information that is relevant to D2D communication and could help "for free" to solve the D2D resource management problems.

The idea set forth in this paper is that, while the cellular channel gains should exhibit fading coefficients that are known to be independent of those measured on the direct channels among the UEs, there actually exists common information between these data at the statistical level. In order to build up the reader's intuition, consider the following toy example. Imagine a green-field (free space) propagation scenario, in which the location of all UEs is made available to the network (even for those devices not interested in communicating with the network), then both the cellular and the D2D channel gains would be easily predictable from the UEs' locations and the use of a deterministic free-space channel

Manuscript received November 15, 2019; revised March 15, 2020 and June 8, 2020; accepted June 28, 2020. Date of publication July 16, 2020; date of current version November 11, 2020. This work was supported in part by the Ministry of Education, Youth and Sports, Czech Republic, under Project LTT18007. The work of David Gesbert was supported in part by HUAWEI-EURECOM Chair on Advanced Mobile Systems towards 6G. The associate editor coordinating the review of this article and approving it for publication was C. Huang. *(Corresponding author: Mehyar Najla.)*

Mehyar Najla, Zdenek Becvar, and Pavel Mach are with the Faculty of Electrical Engineering, Czech Technical University in Prague, 166 36 Prague 6, Czech Republic (e-mail: najlameh@fel.cvut.cz; zdenek.becvar@fel.cvut.cz; machp2@fel.cvut.cz).

David Gesbert is with the Communication Systems Department, EURECOM, 06410 Sophia Antipolis, France (e-mail: gesbert@eurecom.fr).

Color versions of one or more of the figures in this article are available online at http://ieeexplore.ieee.org.

Digital Object Identifier 10.1109/TWC.2020.3008303

model with line of sight (LOS) among all entities. Therefor, in a LOS environment, both D2D and cellular channel gains directly relate to each other via the user location knowledge. In practice, however, the UEs' locations may not be known due to privacy issues or may not be simply available. More importantly, in non-line of sight (NLOS) scenarios (such as suburban or urban areas), the D2D channels and the cellular channels may be obstructed in completely independent manners making the channel prediction from the UEs' locations seemingly impossible. For instance, two devices might experience a strong LOS D2D channel while a building may block the cellular channel between one of these devices (or more) and a given BS, thus making the D2D and cellular channel gains seemingly quite a bit less related than in the pure LOS scenario.

In this paper, we show that, in contrast to initial belief, a hidden and non-explicit relation between the cellular and the D2D channels still exists in the NLOS case, and can be made even stronger by leveraging cellular measurements from additional surrounding BSs. The hidden relation is a result of the dependency of the D2D and cellular channels gains not only on the network topology, but also on the relative locations of the users and the obstacles. Thus, this relation is complex and its derivation is, by its nature, a typical complex model extraction problem, where machine learning is a suitable and efficient solution. Therefore, we exploit a deep neural network (DNN) to extract the complex model for the prediction of the D2D channel gains from the cellular channel gains.

Another interesting by-product of our prediction scheme lies in seeing that the set of cellular gains often constitute an order-of-magnitude smaller dimensional object than the D2D channels that we are trying to predict (i.e., there are just X cellular gains for one cell with X users in it, in contrast to X(X-1) direct and interference D2D gains). Hence, the proposed approach not only offers to capitalize on easier-to-get information (cellular channel estimation) rather than on the harder-to-get D2D channel gains for the optimization of D2D communications, but it also promises substantial savings in signaling for the channel estimation.

In the literature, existing channel prediction works related to this paper typically focus on predicting the channel quality between a single UE and an antenna at the BS at a specific frequency based on either: i) knowing the channel between this UE and the BS antenna at another frequency [22]–[31], or ii) knowing the channel between this BS antenna and another UE that is close to the original UE [32], or iii) knowing the channel between this UE and another close-by antenna at the same BS [33]. However, the problem presented in this paper, which is predicting D2D channel gains based on the cellular channel gains, is of a different nature from the above-mentioned prediction problems solved in the literature because a strong commonality of space can't be relied upon. Note that this paper builds on and extends our previous work presented in [34], where we introduced the idea of the DNN-based prediction of the transmission powers for D2D communication. Instead, in this paper, we generalize the problem to predicting directly the D2D channel gains. This allows for a more powerful framework, which yields applications to various radio resource management (RRM) related optimization problems in D2D networks.

The main contributions of this paper are summarized as follows:

- We present a novel framework for the D2D channel gains prediction based on the cellular channel gains in order to solve various problems related to radio resource management in D2D communication without incurring the pilot overhead that is usually expected in D2D communication.
- We design a DNN to build up a regression model connecting the cellular channel gains (as DNN inputs) to the D2D channel gains (as DNN outputs). The DNN is trained offline via simulations of the targeted area. Thus, the training samples (cellular and D2D channel gains) are collected based on the simulations and, then, used to train the DNN. Our results show a high convergence between the true and the predicted D2D channel gains, even in typical urban NLOS scenarios.
- We demonstrate the efficiency of the proposed framework by applying the predicted D2D gains to existing channel allocation and power control algorithms presented [20] and [21], respectively.
- We analyze the signaling overhead in terms of the number of channel gains needed to implement the radio resource management algorithms from [20] and [21] with and without the proposed DNN-based D2D channel gains prediction scheme to show the benefits of the proposed concept.
- We demonstrate the robustness of the proposed scheme against the environment changes and possible inaccuracies in the simulations of the targeted area during the offline training.

The rest of the paper is organized as follows. In Section II, we present the system model and formulate the problem of D2D channel gains prediction. Then, Section III describes the proposed DNN-based scheme for the prediction of D2D channel gains. Performance evaluation and simulation results are illustrated in Section IV. Finally, Section V concludes the paper.

II. System Model and Problem Formulation

In this section, we present our system model, and then, we formulate the problem of the D2D channel gains prediction.

A. System Model

In our model, we consider L base stations (BSs) deployed randomly in a square area together with U UEs as shown in Fig. 1. The UEs are divided into M CUEs and $2N$ D2D user equipments (DUEs) composing N D2D pairs, hence, $U = 2N + M$. Each D2D pair consists of a transmitter, DUE_T, and a receiver, DUE_R.

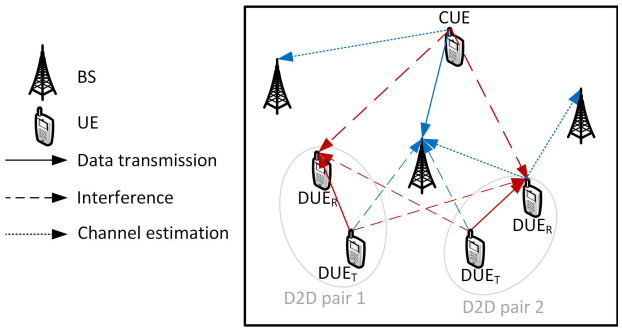

Fig. 1. System model: An example with four DUEs, one CUE and three BSs. Note that red and blue colors are used for D2D and cellular channels, respectively, and only part of the signaling (channel estimation) is shown for sake of clarity.

The capacity of the n-th D2D pair at the k-th communication channel is defined as:

$$C_n^k = B_k log_2 \left(1 + \frac{p_n^k \, g_{n,n}}{B_k \sigma_o + \sum_{\substack{q=1 \\ q \neq n}}^{q=N} p_q^k g_{q,n} + \sum_{m=1}^{m=M} p_m^k g_{m,n}}\right) \quad (1)$$

where, for the k-th channel, B_k is the channel bandwidth, p_n^k is the transmission power of the DUE$_T$ of the n-th D2D pair, p_m^k is the transmission power of the m-th CUE, and p_q^k is the transmission power of the DUE$_T$ of the q-th D2D pair causing interference to the n-th D2D pair (i.e., $q \in \{1, \ldots, N\}/\{n\}$). Further, $g_{n,n}$ represents the channel gain between the DUE$_T$ and the DUE$_R$ of the n-th D2D pair, σ_o is the noise density, $g_{m,n}$ is the interference channel gain between the m-th CUE and the DUE$_R$ of the n-th D2D pair, and $g_{q,n}$ is the interference channel gain between the DUE$_T$ of the q-th D2D pair an the DUE$_R$ of the n-th D2D pair. Note that, without loss of generality, (1) assumes that the noise is an Additive White Gaussian Noise similarly as in [35], [36] and the interference is treated as Gaussian noise. In this paper, the term "channel gain" refers to the magnitude of the channel gain (as in, e.g., [16], [37]), as the magnitude is commonly exploited for, e.g., channel allocation, power control, or to determine the system capacity.

This paper assumes a complete absence of channel gains knowledge among the UEs. Thus, the channel between DUE$_T$ and DUE$_R$ of the same D2D pair, interference channels among DUEs of different D2D pairs, and interference channels among the CUEs and the DUEs (i.e., $g_{n,n}$, $g_{q,n}$, and $g_{m,n}$ in (1)) are unknown.

The DUEs and the CUEs need to estimate uplink/downlink channels to manage efficiently resource allocation and for handover purposes. Thus, although the D2D channel gains are not known by the network, still, the information on the channel quality between each UE (CUE or DUE) and its neighboring BSs are sent periodically to the serving BS in order to update the network information [38]. The corresponding estimated channel gain between any i-th (or j-th) UE and the l-th BS is denoted as $G_{i,l}$ (or $G_{j,l}$). These cellular channel gains ($G_{i,l}$ and $G_{j,l}$) are assumed to be represented by uplink channel gains estimated (measured) by the BS using the common way from the existing reference signals [39]. Nevertheless, it is worth to mention that even downlink channel gains can also be used to estimate quality of cellular channels as the downlink gains can be estimated (measured) by the UEs and fed back to the BS.

B. Problem Formulation

We aim to predict the real (true) channel gain $g_{i,j}$ between any i-th and j-th UEs, that can be, then, exploited for any existing RRM algorithms. Our goal is to minimize the prediction error and we formulate the problem as:

$$\min_{g_{i,j}^*} (g_{i,j} - g_{i,j}^*)^2 \quad (2)$$

where $g_{i,j}^*$ is the predicted channel gain between the i-th and the j-th UEs. To predict the channel gain between any two UEs, we exploit only the available information about each UE, i.e., cellular channel gains. In the next section, we propose a novel DNN-based scheme for the prediction of $g_{i,j}$ relying on the knowledge of the cellular channel gains of the i-th and the j-th UEs.

III. Prediction Scheme

This section describes the proposed scheme for predicting the D2D channel gains. First, we illustrate the principle of the D2D channel gains prediction. Then, we describe the architecture of the proposed DNN and clarify the training process. Moreover, we discuss the signaling overhead reduction reached by the proposed prediction scheme and its implementation aspects.

A. Principle of DNN-Based Prediction of D2D Channel Gains Exploiting Cellular Channel Gains

In general, it is clear that in a green-field (free space) propagation scenario, in which the location of all UEs is made available to the network, both the cellular and the D2D channel gains are easily predictable from the UEs' locations. In the free space area with LOS, the cellular channel from the UE to at least three BSs corresponds to a single specific location of the UE. Consequently, the D2D channel gain value between two UEs can be easily predicted in such (unrealistic) scenario. However, in practice, the UEs' locations may not be known due to privacy issues or may not be simply available. Moreover, in NLOS (urban or suburban) scenarios, the D2D channels and the cellular channels may be obstructed in completely independent manner and the D2D channel prediction from the UEs' locations seems to be impossible. For instance, two devices might experience a strong LOS D2D channel while a building(s) obstructs the cellular channel between one of these devices (or more) and the given BS (see Fig. 2). In such a case, the D2D channel gain between the two UEs might be hard to predict based on the cellular channel gains. However, in contrast to this initial belief, a strong relation between the cellular and the D2D channels is still expected by accounting for additional surrounding BS. The reason behind this is that increasing the number of known cellular channel

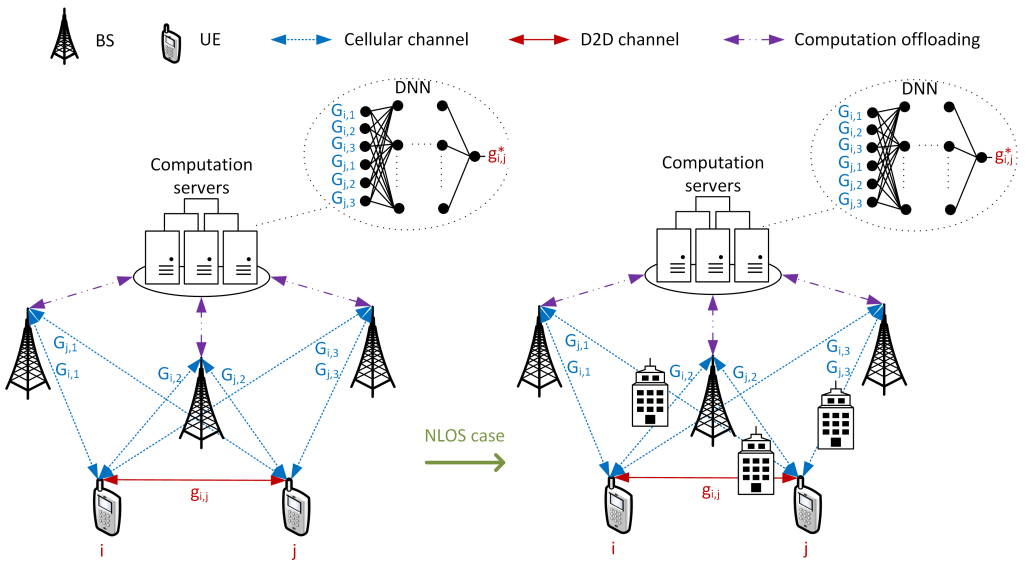

Fig. 2. Illustration of D2D channels prediction based on cellular channels for LOS (left part of figure) and NLOS (right part) scenarios.

gains from each UE leads to a higher confidence related to the UE's location and provides information about the position (and shape) of obstructing elements of the terrain. This information can then, in principle, be mapped into a cartography of D2D gains.

To put the above-mentioned intuition into more rigorous terms, given a specific area with certain topology, terrain and buildings' setup, there exists a mapping $\mathbf{F}$ connecting the cellular channel gains of the existing UEs (denoted as $\mathbf{G^C}$) and the D2D channel gains among these UEs (denoted as $\mathbf{g}$) so that:

$$\mathbf{g} = \mathbf{F}(\mathbf{G^C}) \tag{3}$$

It is obvious that solving the problem (2) can be achieved by approximating the function $\mathbf{F}$ from (3). Nevertheless, this approximation is hard to be done taking into account the changeable size of $\mathbf{G^C}$ and $\mathbf{g}$ when the number of UEs changes. In other words, a different function $\mathbf{F}$ needs to be approximated for every possible number of UEs making the solution unrealistic. Therefore, taking into account the problem defined in (2), we circumvent this problem by approximating the mapping $\mathbf{F}$ between $\mathbf{G^C_{i,j}}$ and $g_{i,j}$ where $\mathbf{G^C_{i,j}} = \{G_{i,1}, \dots G_{i,L}, G_{j,1}, \dots G_{j,L}\}$ includes the gains of the cellular channels from L BSs to any i-th and j-th UEs. In such a way, regardless of the number of the existing UEs, the D2D channel between any two UEs can be predicted by knowing the gains of the cellular channels from these two UEs and the surrounding BSs. hence, the problem (2) is written as:

$$\min_{F}(g_{i,j} - F(\mathbf{G^C_{i,j}}))^2 \tag{4}$$

The optimization problem (4) aims, by approximating F, to minimize the difference between the true (real) and the predicted gains of the D2D channel between any i-th UE and j-th UE; based on the knowledge of the cellular channel gains of these two UEs.

Deep neural networks are typical up-to-date tools for functions approximation and regression models creation. Thus, in this paper, we exploit the DNN to predict $g_{i,j}$ based on $\mathbf{G^C_{i,j}}$.

Note that, for any UE (DUE or CUE), the cellular channel gains between this particular UE and the surrounding BSs are periodically reported to the BSs for purposes related to the conventional communication and/or handover. In addition, in the future mobile networks, the network computations are supposed to be offloaded to powerful computation servers reducing network's energy consumption. Thus, even the proposed DNN can be deployed on these computation servers. The servers collect the estimated cellular channel gains (purple dash-dotted lines in Fig.2) and perform the prediction of $g_{i,j}$. Note that the computation servers can be located at any unit or entity in the network, such as a base station or in the core network. For example, an edge computing server can be exploited. With respect to the conventional architectures of mobile networks (e.g., 4G), the edge computing brings the computing power to the edge of the network where the potential radio resource management algorithms can be run. However, the specific deployment is up to the service provider or the network operator and the prediction should be located as close as possible to the place, where the radio resource management is performed to avoid any additional delay in the radio resource management.

B. The Architecture of the Proposed DNN

The problem of predicting the D2D channel gain between the i-th and the j-th UEs based on the cellular channel gains from both the i-th and j-th UEs to the L BSs is a regression problem, which can be solved by the deep neural network designed to build the regression model. Fig. 3 shows the proposed fully-connected DNN for regression. The proposed DNN is composed of an input layer (X_0), H hidden layers ($X_1, \dots, X_H$) and an output layer (X_{H+1}). The input layer contains the cellular channel gains between the i-th UE and

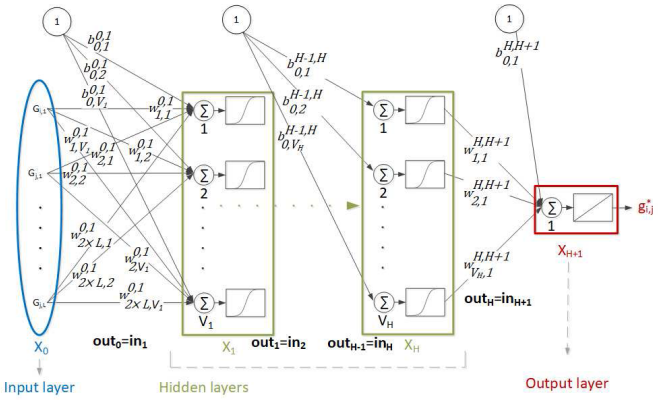

Fig. 3. The proposed DNN to build up a regression model connecting input variables (cellular channel gains from two UEs (i and j) to L BSs) and a single output variable (the D2D channel gain between the i-th and the j-th UE).

the L BSs and between the j-th UE and the L BSs (i.e., $\mathbf{G^C_{i,j}}$) aligned as an input vector in the input layer as illustrated in Fig. 3. Thus, the output of the input layer $\mathbf{out_0}$ is the cellular channel gains vector $\mathbf{G^C_{i,j}} = \{G_{i,1}, \ldots G_{i,L}, G_{j,1}, \ldots G_{j,L}\}$ of length $2 \times L$. Then, the DNN contains H hidden layers whereas every hidden layer X_h is composed of V_h neurons. Every hidden layer X_h has an input vector $\mathbf{in_h}$ equivalent to the output of the previous layer $\mathbf{out_{h-1}}$ (i.e., $\mathbf{in_h} = \mathbf{out_{h-1}}, \forall h \in \{1, \ldots, H\}$). Each input element z in $\mathbf{in_h}$ is fed to every neuron v in the hidden layer X_h with a weight $w^{h-1,h}_{z,v}$. Consequently, every neuron v performs dot product between the input elements in $\mathbf{in_h}$ and the corresponding weights. The result of the dot product is added to a corresponding bias $b^{h-1,h}_{0,v}$ and processed by the commonly used sigmoid function giving the output of the neuron. Hence, the hidden layer X_h with V_h neurons and input vector $\mathbf{in_h}$ gives an output vector $\mathbf{out_h}$ of the length V_h and this output vector $\mathbf{out_h}$ is, thus, written as:

$$\begin{aligned}\mathbf{out_h} &= Sig(\mathbf{W^{h-1,h}in_h} + \mathbf{b^{h-1,h}}) \\ &= Sig(\mathbf{W^{h-1,h}out_{h-1}} + \mathbf{b^{h-1,h}})\end{aligned} \tag{5}$$

where Sig is the sigmoid function $Sig(\mathbf{Z}) = \frac{1}{1+exp(-\mathbf{Z})}$, $\mathbf{W^{h-1,h}}$ is the matrix of weights of the links between every input element of X_h (i.e., equivalent to the output of X_{h-1}) and every neuron in X_h and $\mathbf{b^{h-1,h}}$ is the vector of biases attached to the neurons.

The output of the last hidden layer $\mathbf{out_H}$ is followed by the output layer. The output layer in the DNN for regression of a single variable is composed of one neuron. The single neuron of the output layer performs the dot product between $\mathbf{out_H}$ and the corresponding weights $\mathbf{W^{H,H+1}}$ (i.e., the vector of weights dedicated to the links between the outputs of the last hidden layer X_H and the single neuron in the output layer X_{H+1}). Then, the output layer neuron also sums its attached bias scalar $b^{H,H+1}$ and implements a linear activation function giving an output as:

$$g^*_{i,j} = Lin(\mathbf{W^{H,H+1}out_H} + b^{H,H+1}) \tag{6}$$

where Lin is the linear activation function $Lin(Z) = Z$ and the output $g^*_{i,j}$ of the proposed DNN is the predicted D2D channel gain between the i-th and the j-th UEs.

C. Offline Learning and Exploitation of the Proposed DNN

We propose an offline supervised learning-based solution to predict the D2D channel gain between any two UEs from their cellular channel gains. Actually, the significant benefit of the offline training is that the measurements for the training phase are not needed. Instead, the offline training can be performed by simulations before the channel prediction is adopted for the real world. This offline training process starts with the simulation of the targeted area (e.g., a cell). Within the area, the positions of the UEs, e.g., i and j, are uniformly generated. The cellular channels between the i-th UE and L BSs as well as between the j-th UE and L BSs ($\mathbf{G^C_{i,j}}$) are calculated together with the D2D channels between the i-th and j-th UEs $g_{i,j}$ based on the statistical models of the channel gains. The calculated cellular gains (presenting features) and the D2D gain (presenting the target) compose together a single learning sample. Then, the process is repeated by generating the new positions of the UEs and calculating the channels to constitute new samples. After the samples are collected, the training process is done offline following the typical way used to train any supervised learning-based neural network. In detail, the learning samples are split into a training set and a test set. The samples from the training set are used to train the proposed DNN while the samples in the test set are used to test the accuracy of the trained DNN on a set of samples that is not used for training to prevent overfitting [41]. During the training process, a loss function is defined to evaluate the regression model prediction accuracy. The loss function in the DNN that builds the regression model predicting a single variable is, typically, a measurement showing how far is the predicted value of the variable from the true value of this variable ($g^*_{i,j}$ and $g_{i,j}$ in our case). Therefore, taking the optimization problem (4) into account, we consider a mean square error loss function that can be written as:

$$\iota = \frac{1}{S}\sum_{s=1}^{s=S}(g^s_{i,j} - g^{s*}_{i,j})^2 \tag{7}$$

where S is the number of the training samples, $g^s_{i,j}$ is the target (true D2D channel gain) of the s-th training sample, and $g^{s*}_{i,j}$ is the predicted D2D channel gain based on the cellular channel gains of the s-th training sample.

To minimize the mean square error loss function, the weights and biases of the proposed DNN are updated using Levenberg-Marquardt Backpropagation algorithm, which is an optimization method designed to solve non-linear least squares problems [42]. Thus, Levenberg-Marquardt algorithm can be applied with backpropagation for the neural networks training when the loss function is a sum of squares [43].

The learning steps are done offline based on the samples collected from the simulations of the area with randomly deployed UEs, but without any connection to these specific UEs. The training is focused on obtaining a "mapping" from the cellular channel gains of any two UEs to the channel gain

between these two UEs. Thus, the DNN can learn the general relation between the cellular channels and the D2D channels in the targeted area and the built model is not dedicated to any specific UEs.

After the offline learning is done, the trained DNN is uploaded to the unit where the radio resource management takes place and this DNN is ready to be used in the real mobile network to predict the D2D channel gains between any pair of UEs in the real area. Thus, for multiple UEs, the trained (and tested) DNN is utilized to predict all needed channel gains among every pair of UEs independently and in parallel. To be more specific, based on the cellular channel gains of the UEs, we utilize the trained DNN to obtain all D2D channel gains, such as the channel gains between every two DUEs of the same D2D pair, interference channel gains between every couple of DUEs from different D2D pairs and interference channels between the CUEs and the DUEs. These can be, then, exploited to solve any RRM problem using the existing algorithms.

D. Analysis of Reduction in Signaling Overhead

In this subsection, we discuss the signaling overhead in terms of the number of channel gains that need to be estimated (measured) in the network.

In the existing network, the cellular channel gains between the UEs and the neighboring BSs are commonly estimated (i.e., for conventional communication and handover purposes). The number of the commonly estimated cellular gains is $L(2N + M)$. Note that even the DUEs might need to change from the D2D communication to the conventional communication in the case of a sudden D2D communication quality drop and, therefore, the cellular channels of DUEs are also periodically estimated and reported.

In the literature, for conventional RRM algorithms related to the D2D communication (e.g., power control algorithm from [21]), additional $2N(2N - 1)$ direct and interference D2D channels need to be estimated between the $2N$ DUEs. Moreover, for the D2D in shared mode, interference channels between the CUEs and the DUEs have to be estimated and reported as well. The number of those interference channels between the M CUEs and the $2N$ DUES that should be estimated is $2NM$. Thus, the number of estimated channel gains in the common network with the D2D communication is:

$$\Sigma = L(2N + M) + 2N(2N - 1) + 2NM \tag{8}$$

In this paper, we predict the D2D channel gains from the common estimated cellular gains. In other words, in the network with D2D communication utilizing the proposed prediction scheme, the number of channel gains need to be estimated (measured) is limited to the estimation of $L(2N + M)$ channel gains, which are used to predict the remaining needed D2D channel gains. Thus, by subtracting $L(2N + M)$ from (8), we can calculate the reduction in the number of estimated channel gains. This reduction, in the shared mode, is equal to:

$$\Delta\Sigma = \Sigma - L(2N + M) = 2N(2N - 1) + 2NM \tag{9}$$

In the dedicated mode, the CUEs do not affect the D2D communication as the channels allocated to the CUEs are orthogonal to those allocated to the D2D pairs. In such case, the reduction in the number of estimated channel gains achieved by the proposed prediction scheme is determined by setting M to zero in (8) and (9), respectively.

E. Implementation and Design Aspects

In this subsection, we discuss key implementation and design aspects of the proposed DNN-based prediction of D2D channels.

The first aspect is the number of samples to be collected for the training. The proposed DNN is trained offline. Thus, collecting even a high number of samples (if needed) is feasible, as the samples can be collected by the simulation of targeted area before using the trained DNN in the real world as explained in Section III-C.

Another aspect related to the practical implementation of the prediction scheme is the computational complexity of DNN. In general, the computational complexity of the DNN depends on the number of multiplications done by every neuron in every layer between the inputs of this layer and the corresponding weights. In detail, considering that: 1) the DNN contains H hidden layers with X_H neurons in each layer, 2) the number of DNN inputs is $2L$ (cellular gains between two UEs and L BSs), and 3) the number of DNN outputs is one (the D2D gain between two UEs), then, the number of the multiplications performed for the D2D channel prediction is:

$$\rho = 2LX_1 + \sum_{h=1}^{h=H-1} X_h X_{h+1} + X_H \tag{10}$$

This computational complexity affects the latency with which the channels are predicted in the network. Considering a reasonable number of hidden layers and neurons per each layer (i.e., our DNN includes five hidden layers with 20, 18, 15, 12 and 8 neurons); the number of the performed multiplications (i.e., $\rho = 1034$ multiplications in our DNN when $L = 3$ BSs), consumes a negligible computing time. Hence, we can claim that the latency introduced by the DNN is negligible and the overall delay is (at most) the same as the latency of any other existing centralized approach, within which the D2D channel gains need to be estimated via reference signals, and then reported to the same unit where the DNN is running. Note that with a high number of users, the high signaling in the conventional centralized approaches leads to the need of a high number of reference signals transmitted/received. The high number of the reference signals requires to reserve a lot of resources and can lead to an additional delay due to the channel measurement scheduling. In our case, however, such delay is avoided and the overall delay is reduced to simple multiplications executed by the DNN.

The last practical question is how the proposed prediction scheme copes with RRM algorithms in dynamic environments or scenarios (e.g., moving users, users becoming active/inactive, etc). In such scenarios, disregarding whether our prediction scheme is exploited or not, the RRM algorithm (e.g., channel allocation, power control, etc.) should

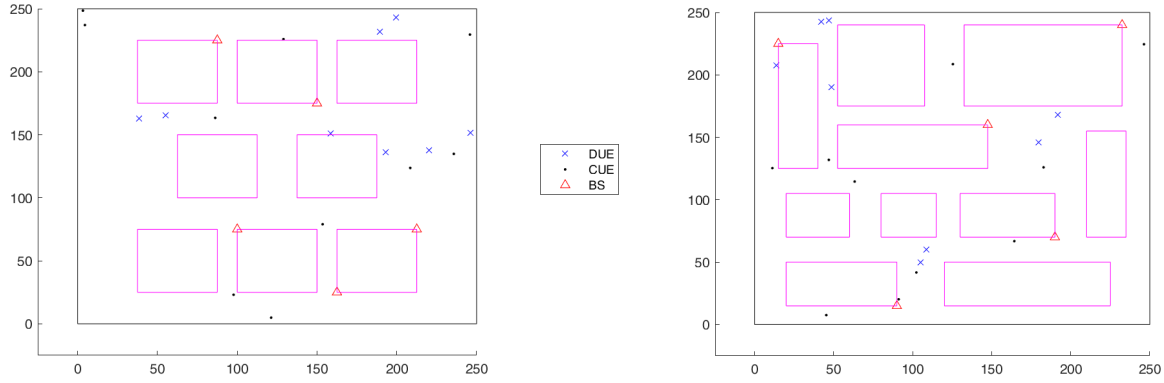

(a) Urban1 (b) Urban2

Fig. 4. Example of simulation deployment with $N = 4$, $M = 10$ and $L = 5$ and several buildings (fixed obstacles) represented by the pink rectangles. Note that the Rural area is of the same size as Urban1/Urban2 without any buildings or obstacles.

be performed periodically. Thus, also the proposed prediction scheme is expected to be repeated periodically to update the predicted D2D channel gains. The predicted D2D channels at each time instant are just inserted as the inputs to the RRM algorithms and every DUE is told to change its communication parameters (e.g., the channels the DUE is occupying, the DUE's transmission power at every channel, etc).

IV. Performance Evaluation

In this section, we describe the simulation scenarios and parameters, and then, we discuss simulation results from three different perspectives as follows. First, we analyze the accuracy of the prediction scheme statistically showing how close the predicted D2D channel gains are to the true gains of the D2D channels. Second, we illustrate the performance of the proposed prediction scheme on selected examples of existing algorithms for D2D RRM in the mobile network, and we show how this prediction scheme affects the D2D communication quality and network's signaling overhead. The proposed prediction scheme aims to reduce the signaling overhead needed for D2D communication without significant losses in the communication quality. Last, we evaluate the robustness of the proposed scheme against the environment changes and the potential inaccuracies in the simulations during the training phase.

A. Simulation Scenarios and Performance Metrics

We consider up to 20 DUEs (composing up to 10 D2D pairs) and 10 CUEs deployed uniformly within an area of 250×250 m^2 covered by up to 5 BSs. Although the DUEs are uniformly distributed, the maximum distance between the DUE_T and the DUE_R of the same D2D pair is upper-bounded by a maximal distance of $d_{max} = 50$ m as in [44], [45] to guarantee the availability of D2D communication. For any D2D transmitter, the maximal and the minimal transmission powers are set to $p_{max} = 24$ dBm and $p_{min} = 1$ dBm, respectively, like in [34].

We consider three different scenarios according to the signal propagation between the UEs and the BSs and among all UEs. The first scenario assumes an open rural area denoted as Rural with a full availability of line-of-sight (LOS) for all channels (D2D channels and cellular channels). The other two scenarios, illustrated in Fig. 4a and Fig. 4b, correspond to two different urban areas (such as scenario C2 in [46]) with fixed obstacles (FOs) representing e.g., buildings, and we denote these two urban areas as Urban1 and Urban2. In Urban1 and Urban2, the buildings lead to a certain probability of non-line-of-sight (NLOS) for both the D2D and cellular channels. Note that two different urban areas are simulated to validate our prediction approach for different buildings topologies without any changes in the DNN architecture.

In all areas, Rural, Urban1 and Urban2, the LOS path loss is generated in line with 3GPP recommendations [47]. In the urban areas, we assume that the communication channel intercepted by a single or more building walls is exposed to an additional loss of 10 dB per wall as in [34]. Note that Fig. 4 presents a 2D projection of the simulated urban areas, nevertheless, in our simulations, the building heights are distributed uniformly between 20 and 30 m to randomly affect NLOS and LOS probabilities. Simulation parameters are summarized in Table I.

For the learning process, we collect 1 000 000 samples. Note that obtaining such a number of samples is feasible, as the training process is done offline by the simulations. Still, we also study the impact of the number of learning samples on the prediction accuracy in the next subsection. The samples are then divided into samples used for DNN training (70% of samples are used as the training set) and 30% of samples are for the testing (i.e., the test set).

The proposed DNN exploits five hidden layers composed of 20, 18, 15, 12, and 8 neurons, respectively. The number of hidden layers and the number of neurons in each layer are set by trial and error approach. These specific numbers of hidden layers and neurons are tested for the case when the number of the DNN inputs is $2 - 10$ (i.e., the cellular channels between two UEs and $1 - 5$ BSs); and for three areas

TABLE I
SIMULATION PARAMETERS

Parameter		Value
Carrier frequency	f_c	2 GHz
Bandwidth	B	20 MHz
Number of D2D pairs	N	2 – 10
Number of CUEs (shared mode only)	M	10
Number of channels (shared mode only)	K	10
Bandwidth per any k-th channel (shared mode only)	B_k	2 MHz
Maximal distance between DUE_T and DUE_R of the same pair	d_{max}	50 m
Number of BSs	L	1 – 5
Maximal transmission power	p_{max}	24 dBm [34]
Minimal transmission power	p_{min}	1 dBm [34]
Noise power spectral density	σ_o	−174 dBm/Hz

(Rural, Urban1, and Urban2). Thus, as the number of DNN's outputs is always fixed to one (a single D2D channel gain is being predicted), this number of hidden layers and neurons is expected to be suitable for learning the relation between the cellular gains and the D2D channel gains in different areas.

In this paper, we evaluate the proposed prediction scheme from following perspectives:

$i)$ Statistical evaluation of the prediction accuracy before implementing the prediction scheme in the mobile network. For the statistical evaluation, we consider the well-known Pearson correlation coefficient as a performance metric to show the accuracy of the predicted D2D channel gains with respect to the true channel gains. The Pearson correlation coefficient values range between zero and one where the value of one represents a complete matching between the predicted and the true values of the D2D channel gains.

$ii)$ Performance of the D2D communication with the proposed prediction. The performance is represented by the sum capacity of the D2D pairs: $C = \sum_{n=1}^{n=N} \sum_{k=1}^{k=K} C_n^k$ and by the signaling overhead corresponding to the number of channel gains to be estimated/reported in the network.

$iii)$ Robustness of the proposed scheme to identify the impact of potential inaccuracies between the simulations of the targeted area for training and the actual real-world area and the resistance to the changes in the real-world environment.

The three above-mentioned evaluation perspectives are presented in the next subsections.

B. Statistical Analysis of the Prediction Scheme

In this subsection, we analyze the results related to $g_{i,j}$ prediction statistically. In other words, as the training is done offline before its usage in the mobile network, we aim to study the prediction accuracy from the statistical point of view showing how close we expect the predicted gain of a D2D channel to be compared to the true gain of this channel. We show the statistical results of predicting a single D2D channel gain by testing the trained DNN on the test set.

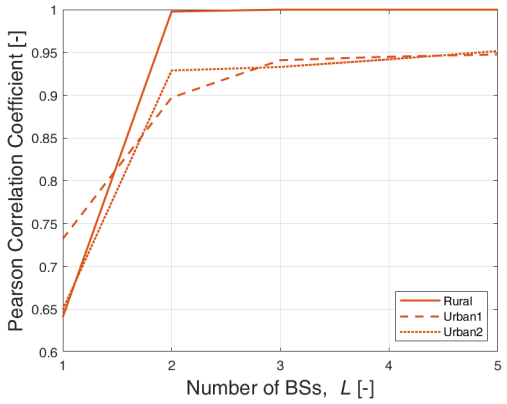

Fig. 5. Pearson correlation coefficient between the true and the predicted D2D channel gains versus number of BSs L.

Fig. 5 shows Pearson correlation coefficient between true and predicted D2D channel gains over different number of BSs. As expected, the Pearson correlation coefficient increases with the number of BSs in all areas. In detail, for the Rural area, a single BS is not enough to extract a well-performing relation between the cellular and the D2D gains (i.e., the Pearson correlation coefficient is around 0.64 for the Rural area when one BS is available). Then, when two or more BSs exist, the Pearson correlation coefficient in the Rural area reaches almost a perfect value (i.e., 0.999). For the urban areas, the Pearson correlation coefficient values are, in general, similar and the difference between Urban1 and Urban2 decreases for a higher number of the BSs. For only one BS, the correlation coefficients for both urban areas vary by about 0.09 due to the effect of the BSs location and the fixed obstacles' (i.e., buildings) locations. Then, already for two BSs, the difference is only below 0.03, and for three BSs, the Pearson correlation coefficients are almost the same for both areas (the difference is less than 0.01). We see, in Fig. 5, that for three or more BSs the correlation coefficient almost saturates for both urban areas reaching, approximately, their maximal values. Note that the Pearson correlation coefficient achieved by the urban areas (i.e., around 0.95) is lower compared to the Rural area (i.e., 0.999) because the cellular channel gains are less random in the Rural area where the buildings are absent and only LOS channels are present.

Fig. 6 shows the regression plot for Rural (Fig. 6a), Urban1 (Fig. 6b), and Urban2 (Fig. 6c) with $L = 3$ BSs and considering $1\ 000$ testing samples from the test set. In general, we see that the values of the path loss in the urban areas are spread in a wider domain compared to the Rural area. This is because of the presence of the FOs and, thus, also NLOS links as explained in Section IV-A. Note that the path loss values in the Urban2 area are spread a little bit more (up to 220 dB) comparing to the Urban1 area

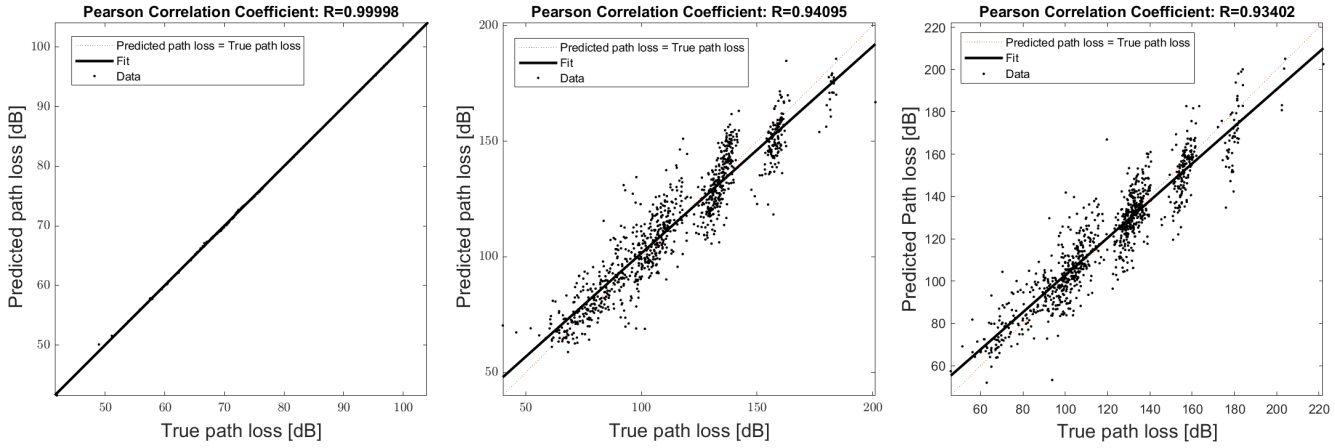

(a) Rural (b) Urban1 (c) Urban2

Fig. 6. Regression plot for $L = 3$ BSs.

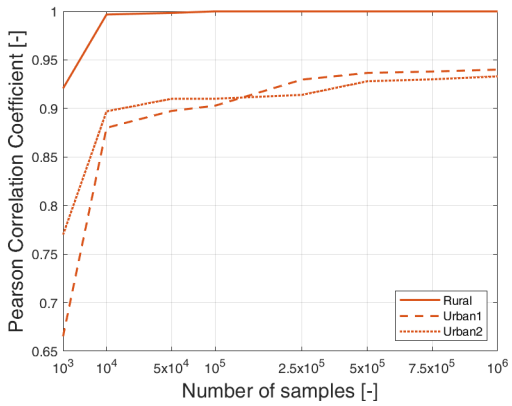

Fig. 7. Pearson correlation coefficient between the true and the predicted D2D channel gains versus number of learning samples for $L = 3$ BSs.

(up to 200 dB) as the former one contains more FOs than the latter one. We can also see, in Fig. 6a, that the predicted path loss (i.e., $10log_{10}(1/g^*_{i,j})$) matches almost perfectly the true path loss (i.e., $10log_{10}(1/g_{i,j})$) for the Rural area. However, some deviation of the predicted path losses from the true values can be seen in Fig. 6b and Fig. 6c in both urban areas. This deviation is a result of the existence of the FOs producing some randomness and uncertainty in the values of the estimated channel gains. Nevertheless, the predicted and the true path losses are, still, highly correlated and Pearson correlation coefficient equals 0.94 and 0.934 for the Urban1 and Urban2 areas, respectively. Actually, the reached Pearson correlation coefficient in the Urban2 area is almost the same as that for Urban1 area(the difference is about 0.006).

Note that results presented in Fig. 5 and Fig. 6 are based on learning with $1\ 000\ 000$ samples. Consequently, to illustrate the influence of the number of samples on the learning accuracy, Fig. 7 shows Pearson correlation coefficient over number of samples for the Rural and both of the urban areas. In all areas, the correlation coefficient increases with the number of samples rapidly at the beginning for lower numbers of the samples. Then, the correlation coefficient increment with the number of learning samples becomes negligible and the Pearson correlation coefficient saturates to (almost) a fixed maximal value. We further see that, in the Rural area, $10\ 000$ samples are sufficient to reach almost a perfect matching between the predicted and the true D2D channel gains. For both urban areas, more samples should be collected due to the higher difficulty of constructing the regression model that connects the cellular channel gains to the D2D channel gains if the FOs are present and randomize the path loss. In detail, Fig. 7 illustrates that the values of the Pearson correlation coefficient in the Urban2 area are higher compared to the Urban1 area for low number of samples. This is explained by the fact that the outdoor space is smaller in the Urban2 and, thus, fewer learning samples (compared to the Urban1) can give a clearer idea about the general relation between the cellular and the D2D gains. Thus, the Pearson correlation coefficient is closer to the saturation value in the Urban2 area with respect to the Urban1 area for low number of samples. However, with the increasing number of samples, the DNN used for the Urban1 starts to learn the topology of the area and the Pearson correlation coefficient increases and saturates to a final value that is slightly higher than the one reached in the Urban2 area. The reason is that the higher number of FOs in the Urban2 makes it harder for the DNN to memorize the corresponding network topology and to extract the relation between the cellular and the D2D gains. Notice that, for both urban areas, even $10\ 000$ samples are enough to reach correlation coefficients above 0.88.

In Fig. 8, we show the effect of the possible noise and inaccuracy in the estimation (measurement) of the conventional cellular channels by the BSs. To this end, we define SNR_G as zero-mean Gaussian noise (i.e., the error) added to the modeled cellular channel gain estimation. Hence, SNR_G represents the cellular channel gain estimation accuracy and it is expressed as the ratio between the true cellular channel gain (UE to BS) and the noise representing an error in estimation of the UE to BS channel. Thus, we add the

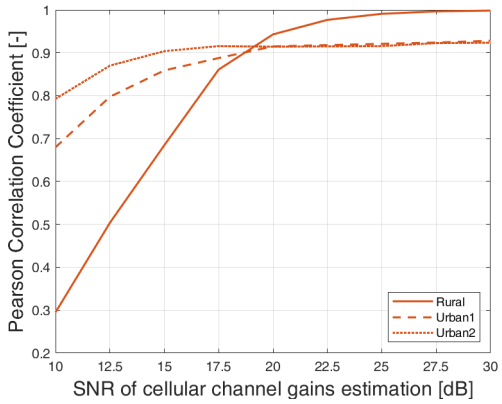

Fig. 8. Pearson correlation coefficient between the true and the predicted D2D channel gains versus the cellular channel estimation accuracy represented via estimation SNR ($L = 3$BSs).

noise of $\mathcal{N}(0, e)$ (where $SNR_G = 10log_{10}(\frac{G_{i,l}}{e})$ dB) to the estimated cellular channel gain $G_{i,l}$. Fig. 8 shows that, with the increasing accuracy of the estimated cellular channels, the correlation coefficient between the true and predicted D2D channel gains increases gradually until the saturation is reached when SNR_G is equal to 25 dB, 20 dB, and 17.5 dB for the Rural, Urban1, and Urban2 areas, respectively. This is, however, an interesting behaviour where a higher probability of LOS leads to a higher sensitivity of the prediction scheme to the channel estimation noise. Consequently, the trained model for the D2D channel prediction in the Rural area is more sensitive to the channel estimation noise than the trained model for the Urban1 area. Similarly, the trained model for the D2D channel prediction in the Urban1 area is more sensitive to the channel estimation noise than the trained model for the Urban2 area. The reason is that, in the Urban2 area, more space is occupied by the FOs (i.e., buildings) compared to the Urban1 area, while the Rural area contains no FOs (i.e., the LOS probability in the Rural area is higher than in the Urban1 area, and the LOS probability of the Urban1 area is higher than in the Urban2 area).

C. Performance of D2D Communication Aided by the Prediction Scheme

In this subsection, we show the impact of exploiting the proposed D2D channel prediction scheme based on machine learning for the D2D communication in the mobile network. For this purpose, we adopt two up-to-date RRM algorithms, one for the channel allocation in the D2D shared mode [20] and one greedy algorithm for a binary power control in the D2D dedicated mode [21]. For both algorithms, we compare the performance (i.e., sum capacity of D2D pairs and the number of channels need to be estimated) in the case when these algorithms are supported by our proposed D2D channel prediction scheme with the case when these algorithms are implemented without the machine learning-based prediction approach according to the respective original papers [20] and [21]. The purpose of this comparison is to show that the performance of the existing RRM schemes reached with the proposed prediction scheme is not impaired while a substantial reduction in signaling overhead is achieved. Note that, in the legend of this subsection's figures, CA and PC are used to denote channel allocation scheme from [20] in the shared mode and binary power control from [21] in the dedicated mode.

Fig. 9a shows the sum capacity of D2D pairs over the number of D2D pairs communicating in the shared mode and with the channel allocation scheme from [20] implemented on the true and the predicted D2D channel gains. Fig. 9a illustrates that, by comparing the sum capacity reached when the true D2D gains are known and when the predicted D2D channel gains are used, the capacity loss induced by the prediction scheme reaches 0%, 4%, and 6% for the Rural, Urban1, and Urban2, respectively. This behavior is expected as the Rural area contains no FOs and our prediction scheme reaches a higher Pearson correlation coefficient in this Rural area comparing to the Urban1 and Urban2 areas. Moreover, the Urban1 area contains less FOs and our prediction scheme reaches a slightly higher Pearson correlation coefficient in the Urban1 than in the Urban2, thus a lower gap in the sum capacity between the true and the predicted gains is achieved in the Urban1 area.

Note that, In Fig. 9a, the changes of the sum capacity of D2D pairs over different numbers of D2D pairs, in all areas, follows the behavior described in [20].

The performance of the greedy algorithm for binary power control in D2D dedicated mode from [21] is shown in Fig. 9b, where the D2D pairs are considered to reuse the whole bandwidth. Then, the greedy algorithm is implemented to make a binary transmission power decision for each D2D pair with true and predicted D2D channel gains. In the Rural area, a perfect matching between the binary power control implemented on true and on predicted gains is achieved due to the very high accuracy in the prediction of the D2D channel gains. In the urban areas, only a small loss in the sum capacity, ranging from 1% (for two pairs) to 9% (for ten pairs) in both the Urban1 and the Urban2 areas, is introduced by implementing the binary power control on the predicted D2D channel gains comparing to the binary power control based on the true gains. However, such a loss can be expected by the fact that making a binary decision about the transmission power of each D2D pair is critical and highly sensitive to the accuracy of the predicted D2D channel gains. Nevertheless, ten D2D pairs in proximity reusing a single channel is an extreme case that is not expected to occur often in the real network. In contrast, a reasonable case is when, approximately, four or six D2D pairs reuse a single channel. For instance, with four D2D pairs, the binary power control implemented on the predicted D2D channel gains loses only 2.9% and 3.9% in the Urban1 and Urban2 areas, respectively, comparing to the binary power control with full knowledge of the true D2D channel gains. Such small difference between the Urban1 and the Urban2 areas is understandable as the Urban1 area contains less FOs, and our prediction scheme reaches a slightly higher Pearson correlation coefficient in the Urban1 area than in the Urban2 area.

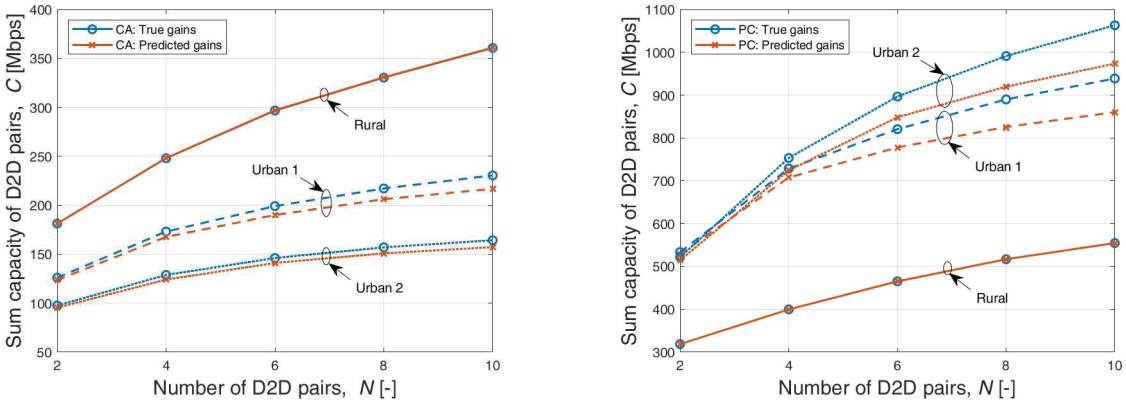

(a) Channel allocation (b) Power control

Fig. 9. Sum capacity of D2D pairs versus number of D2D pairs when channel allocation scheme from [20] for D2D shared mode (a), and binary power control algorithm from [21] for D2D dedicated mode (b), are implemented on the true and the predicted D2D channel gains ($L = 3$ BS and $M = 10$ CUEs).

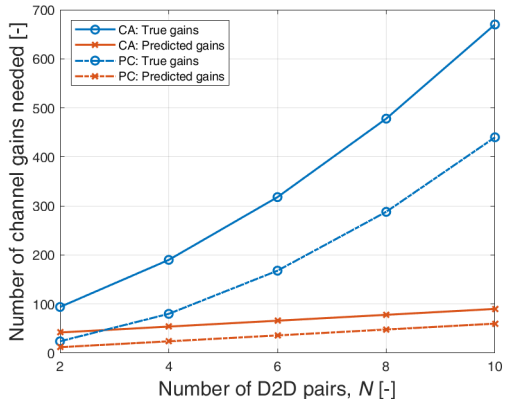

Fig. 10. Signaling overhead in terms of number of channels need to be estimated by the network versus number of D2D pairs; when channel allocation scheme from [20] or binary power control from [21] is implemented on true and predicted D2D channel gains ($L = 3$ BS and $M = 10$ CUEs).

Note that, In Fig. 9b, the changes of the sum capacity of D2D pairs over different numbers of D2D pairs, in all areas, follow the behavior described in [21].

In Fig. 10, we show the signaling overhead in terms of the number of channels estimated by the network if the channel allocation scheme from [20] and the greedy algorithm for binary power control from [21] are implemented on true and predicted D2D channel gains. As shown in Fig. 10, for both the channel allocation scheme from [20] and the power control algorithm from [21], the number of estimated channel gains with the proposed prediction scheme is significantly lower than when all the channel gains would need to be estimated. More specifically, we need to estimate/report up to approximately seven times less channel gains if the proposed DNN-based prediction is used for the channel allocation scheme from [20] or the power control algorithm from [21] comparing to the case when the knowledge of all gains would be required.

D. Robustness of the Proposed Scheme

In this subsection, we analyze the robustness of the proposed scheme when the offline simulation-based trained DNN is used to predict the D2D channel gains in the real-world environment that differs from the simulated area used for training or if the real-world environment changes.

First, we study the impact of moving obstacles', MOs, presence in the real-world urban area(s) on the proposed prediction scheme as the presence and the movement of these MOs is not captured during the offline training by means of simulations. In this respect, up to 30 MOs representing, e.g., vehicles or position-changing obstacles, are uniformly distributed outdoor in both urban areas (see Fig. 11). The dimensions of each MO and its attenuation are also uniformly generated such that the length of the MO is between 2 and 6 m, the width varies from 0.5 to 2 m, the height is from 1.5 to 3 m, and the attenuation varies between 1 and 5 dB. Note that all above-mentioned values are regenerated randomly in every simulation drop.

In Fig. 12, we analyze the effect of the MOs on the channel allocation algorithm from [20] and the binary power control algorithm from [21] while four D2D pairs are considered. As expected, the difference between the sum capacity when the D2D true channel gains are known and the case when the prediction scheme is exploited, increases with the number of MOs in the area. This is due to the signal attenuation differences induced by the MOs' presence in the environment with respect to the training one simulated without those MOs. Particularly, for the channel allocation and with 30 MOs in the area, the additional capacity losses are 2.4% ($5.7\% - 3.3\%$) and 0.6% ($3.8\% - 3.2\%$) for the Urban1 and Urban2 areas, respectively (see Fig. 12a). In the case of power control (Fig. 12b), the additional capacity losses for 30 MOs in the area are 2% ($5\% - 3\%$) and 0.4% ($4.4\% - 4\%$) for the Urban1 and Urban2 areas, respectively. Such low losses are acceptable considering the fact that no specific D2D channel measurements are required and, still, the D2D communication can be enabled due to our proposed channel prediction.

Fig. 12 also shows that the prediction scheme is more sensitive to the MOs' existence in the Urban1 area compared to the Urban2 area. In fact, this is in line with Fig. 8, which shows that the higher ratio of LOS communication in the

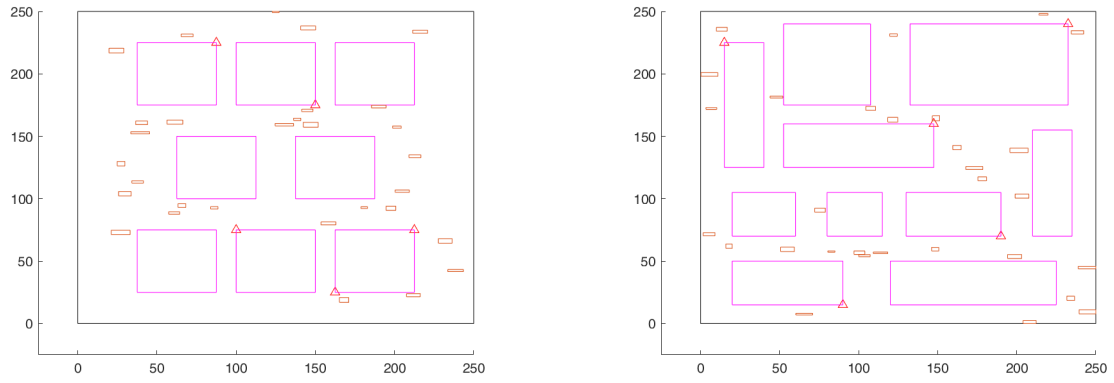

(a) Urban1 (b) Urban2

Fig. 11. Example of simulation deployment with 30 vehicles (moving obstacles) represented by the orange elements, in addition to the buildings (fixed obstacles) represented by the pink rectangles. Note that the red triangles represent the BSs.

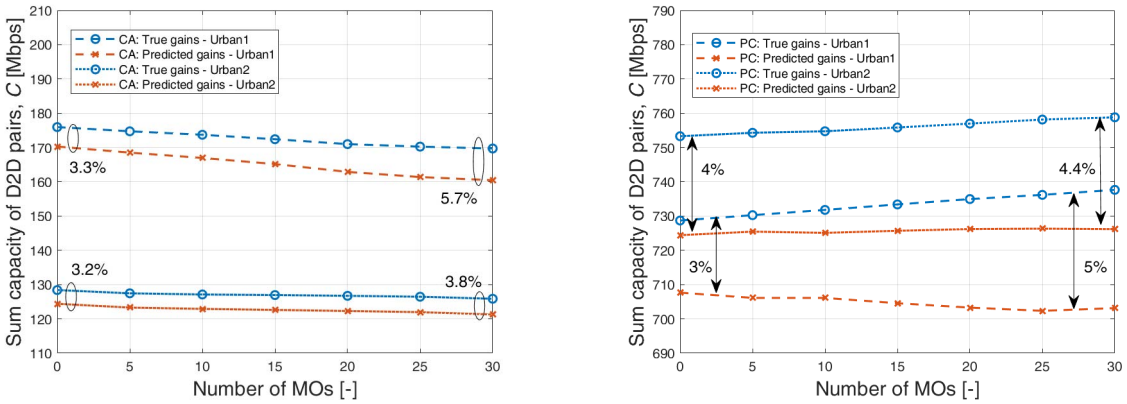

(a) Channel allocation (b) Power control

Fig. 12. Effect of the vehicles (moving obstacles) for four D2D pairs, $N = 4$.

area (i.e., the lower number of obstacles) leads to a higher sensitivity to the noise in the channel gains estimation. Note that the attenuation added by the MOs can be considered as noise because its unpredictable. Hence, the MOs presence affects the Urban1 area more than the Urban2 area, as the Urban1 contains a larger area where LOS communication is possible due to the smaller space occupied by the buildings.

Second, we test the case when the trained DNN is utilized in the urban areas with changed volumes of the buildings (i.e., the fixed obstacles, FOs), see Fig. 13. In our evaluation, the volume of every FO can either increase (the probability of this is set to 0.5) or decrease (the probability of this is also set to 0.5). Then, the percentage of the changes in the volume of every FO is randomly generated so that the average change in the FOs' volume is fixed and corresponds to the targeted value of the change in order to present the results in the figures (i.e., the x axis in Fig. 14 represents the average change in the volumes of the FOs). We consider that the average percentage of FO's change is up to 25% and, without loss of generality, the change in the volume of any FO is divided equally over its three dimensions (i.e., length, width, and height). For instance, if the FO's volume decreases by 25%, every dimension of this FO is decreased by approximately 9%. Fig. 13 shows an example of the real Urban1 and Urban2 areas after the changes in the volumes of FOs' with respect to the simulated volumes of the FOs that are used for training.

In Fig. 14, we show the effect of the changes in the volumes of the FOs on the channel allocation algorithm from [20] and the binary power control algorithm from [21] in both urban areas and with four D2D pairs. Similar to the MOs case, the sum capacity reached when the proposed prediction scheme is exploited modestly decreases comparing to the case when the D2D true channel gains are known. This decrease is slightly more notable for larger changes in the volumes of the FOs as expected. However, the capacity decrease induced by the FOs' volume changes is only up to 2.1% ($5.5\%-3.4\%$) and 1.4% ($5\%-3.6\%$) in the case of channel allocation (Fig. 14a) for the Urban1 and Urban2 areas, respectively. Similarly, the power control (Fig. 14b) is affected only negligibly by up to only 1.8% ($5\%-3.2\%$) and 1.1% ($4.9\%-3.8\%$) for the Urban1 and Urban2 areas, respectively. Comparing the sensitivity of the Urban1 and Urban2 areas to the changes in the volume of FOs, we see that the Urban1 area is slightly more sensitive to the changes in the FOs' volumes. This is,

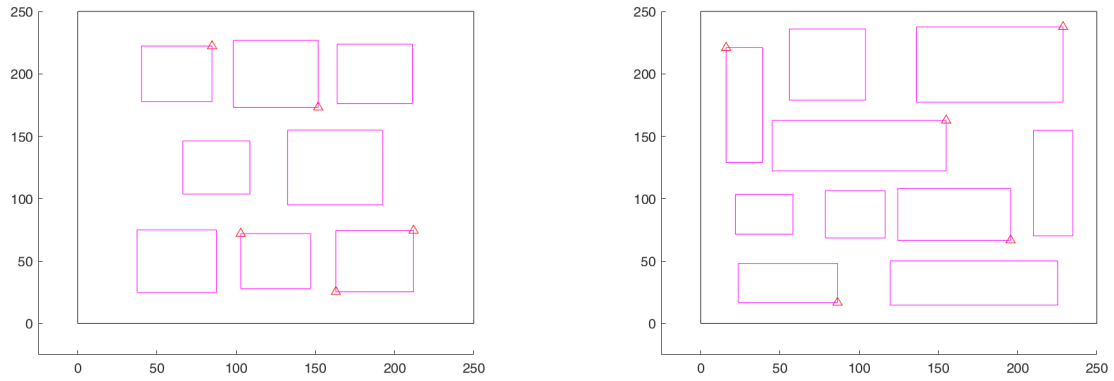

(a) Urban1 (b) Urban2

Fig. 13. Example of simulation deployment with a 25% average change in the volumes of the buildings (fixed obstacles) represented by the pink rectangles, compared to their volumes in Fig. 4. Note that the red triangles represent the BSs.

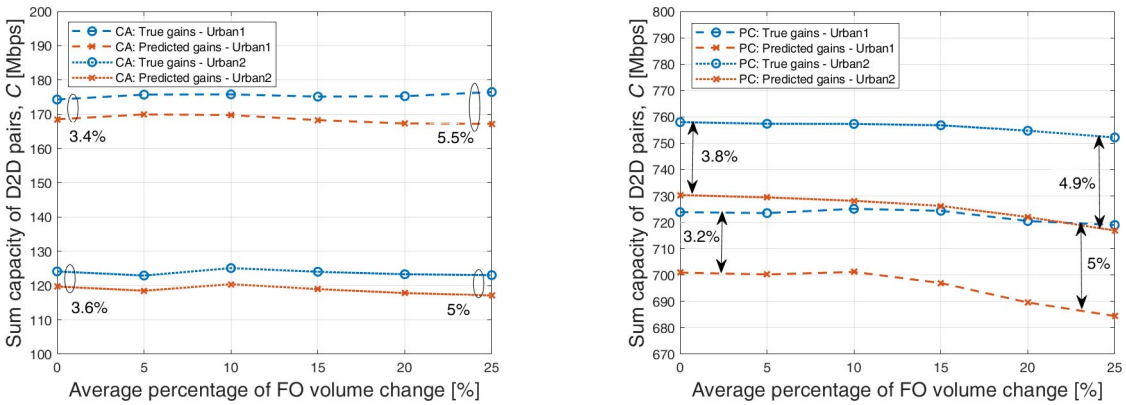

(a) Channel allocation (b) Power control

Fig. 14. Effect of the changes in the volumes of the buildings (fixed obstacles) for four D2D pairs, $N = 4$.

however, expected due to the higher influence of the channel estimation noise on the Urban1 area, which is a result of the higher LOS probability compared to the Urban2 area as explained for the MOs.

These encouraging results, confirm the robustness of the proposed prediction scheme against the changes in the real-world environment and the potential inaccuracies in the training phase.

V. Conclusion

In this paper, we have proposed a novel D2D channel gains prediction scheme based on the cellular channel gains between the UEs and multiple BSs. The proposed prediction scheme takes the advantage of the network topology-related correlation between the cellular and D2D channel gains. Supervised learning-based approach exploiting deep neural networks has been implemented to extract the mapping between the cellular channel gains of any couple of the UEs (i.e., gains of channels between these two UEs and multiple BSs) and the gain of the D2D channel between these two UEs. The proposed prediction scheme achieves a high Pearson correlation coefficient between the true and the predicted D2D channel gains. In addition, we show that the proposed prediction scheme significantly reduces the networks' signaling (represented by channel state information) overhead if applied to realistic radio resource management algorithms. This saving of the channel information is at the cost of only a negligible performance losses in terms of communication capacity comparing to the conventional implementation of these algorithms with knowledge of all channels. We have also demonstrated that the proposal is robust and resilient to the possible changes in the environment induced by various moving obstacles or potential changes in the fixed obstacles (e.g., the buildings) that exist in the area.

The future work should focus on improving the prediction scheme performance (prediction accuracy) for scenarios with buildings and obstacles existence. Moreover the future work should include studying the proposed prediction scheme performance for more RRM algorithms and in different possible scenarios and cellular cell types.

References

[1] M. N. Tehrani, M. Uysal, and H. Yanikomeroglu, "Device-to-device communication in 5G cellular networks: Challenges, solutions, and future directions," *IEEE Commun. Mag.*, vol. 52, no. 5, pp. 86–92, May 2014.

[2] P. Mach, Z. Becvar, and T. Vanek, "In-band device-to-device communication in OFDMA cellular networks: A survey and challenges," *IEEE Commun. Surveys Tuts.*, vol. 17, no. 4, pp. 1885–1922, 2015.

[3] P. Mach, Z. Becvar, and M. Najla, "Combined shared and dedicated resource allocation for D2D communication," in *Proc. IEEE 87th Veh. Technol. Conf. (VTC Spring)*, Jun. 2018, pp. 1–7.

[4] F. H. Khan, Y.-J. Choi, and S. Bahk, "Opportunistic mode selection and RB assignment for D2D underlay operation in LTE networks," in *Proc. IEEE 79th Veh. Technol. Conf. (VTC Spring)*, May 2014, pp. 1–5.

[5] Y. Huang, A. A. Nasir, S. Durrani, and X. Zhou, "Mode selection, resource allocation, and power control for D2D-enabled two-tier cellular network," *IEEE Trans. Commun.*, vol. 64, no. 8, pp. 3534–3547, Aug. 2016.

[6] J. Kim, S. Kim, J. Bang, and D. Hong, "Adaptive mode selection in D2D communications considering the bursty traffic model," *IEEE Commun. Lett.*, vol. 20, no. 4, pp. 712–715, Apr. 2016.

[7] D. Ma, N. Wang, and X. Mu, "Resource allocation for hybrid mode device-to-device communication networks," in *Proc. 8th Int. Conf. Wireless Commun. Signal Process. (WCSP)*, Oct. 2016, pp. 1–5.

[8] Y. Li, M. C. Gursoy, and S. Velipasalar, "Joint mode selection and resource allocation for D2D communications under queueing constraints," in *Proc. IEEE Conf. Comput. Commun. Workshops (INFOCOM WKSHPS)*, Apr. 2016, pp. 490–495.

[9] F. Jiang, B. Wang, C. Sun, Y. Liu, and R. Wang, "Mode selection and resource allocation for device-to-device communications in 5G cellular networks," *China Commun.*, vol. 13, no. 6, pp. 32–47, Jun. 2016.

[10] S. Shamaei, S. Bayat, and A. M. A. Hemmatyar, "Interference management in D2D-enabled heterogeneous cellular networks using matching theory," *IEEE Trans. Mobile Comput.*, vol. 18, no. 9, pp. 2091–2102, Sep. 2019.

[11] S. M. A. Kazmi *et al.*, "Mode selection and resource allocation in device-to-device communications: A matching game approach," *IEEE Trans. Mobile Comput.*, vol. 16, no. 11, pp. 3126–3141, Nov. 2017.

[12] T. Huynh, T. Onuma, K. Kuroda, M. Hasegawa, and W.-J. Hwang, "Joint downlink and uplink interference management for device to device communication underlaying cellular networks," *IEEE Access*, vol. 4, pp. 4420–4430, 2016.

[13] Y. Gu, Y. Zhang, M. Pan, and Z. Han, "Matching and cheating in device to device communications underlying cellular networks," *IEEE J. Sel. Areas Commun.*, vol. 33, no. 10, pp. 2156–2166, Oct. 2015.

[14] R. Wang, J. Zhang, S. H. Song, and K. B. Letaief, "QoS-aware joint mode selection and channel assignment for D2D communications," in *Proc. IEEE Int. Conf. Commun. (ICC)*, May 2016, pp. 1–6.

[15] R. AliHemmati, B. Liang, M. Dong, G. Boudreau, and S. H. Seyedmehdi, "Power allocation for underlay device-to-device communication over multiple channels," *IEEE Trans. Signal Inf. Process. Over Netw.*, vol. 4, no. 3, pp. 467–480, Sep. 2018.

[16] R. AliHemmati, M. Dong, B. Liang, G. Boudreau, and S. H. Seyedmehdi, "Multi-channel resource allocation toward ergodic rate maximization for underlay device-to-device communications," *IEEE Trans. Wireless Commun.*, vol. 17, no. 2, pp. 1011–1025, Feb. 2018.

[17] Y. Qian, T. Zhang, and D. He, "Resource allocation for multichannel device-to-device communications underlaying QoS-protected cellular networks," *IET Commun.*, vol. 11, no. 4, pp. 558–565, Mar. 2017.

[18] R. Yin, C. Zhong, G. Yu, Z. Zhang, K. K. Wong, and X. Chen, "Joint spectrum and power allocation for D2D communications underlaying cellular networks," *IEEE Trans. Veh. Technol.*, vol. 65, no. 4, pp. 2182–2195, Apr. 2016.

[19] W. Lee, M. Kim, and D.-H. Cho, "Deep power control: Transmit power control scheme based on convolutional neural network," *IEEE Commun. Lett.*, vol. 22, no. 6, pp. 1276–1279, Jun. 2018.

[20] P. Mach, Z. Becvar, and M. Najla, "Resource allocation for D2D communication with multiple D2D pairs reusing multiple channels," *IEEE Wireless Commun. Lett.*, vol. 8, no. 4, pp. 1008–1011, Aug. 2019.

[21] A. Gjendemsjo, D. Gesbert, G. E. Oien, and S. G. Kiani, "Binary power control for sum rate maximization over multiple interfering links," *IEEE Trans. Wireless Commun.*, vol. 7, no. 8, pp. 3164–3173, Aug. 2008.

[22] T. Aste, P. Forster, L. Fety, and S. Mayrargue, "Downlink beamforming avoiding DOA estimation for cellular mobile communications," in *Proc. IEEE Int. Conf. Acoust., Speech Signal Process. (ICASSP)*, vol. 6, May 1998, pp. 3313–3316.

[23] K. Hugl, J. Laurila, and E. Bonek, "Downlink beamforming for frequency division duplex systems," in *Proc. Seamless Interconnection Universal Services. Global Telecommun. Conf.*, vol. 4, Dec. 1999, pp. 2097–2101.

[24] Y.-C. Liang and F. P. S. Chin, "Downlink channel covariance matrix (DCCM) estimation and its applications in wireless DS-CDMA systems," *IEEE J. Sel. Areas Commun.*, vol. 19, no. 2, pp. 222–232, 2001.

[25] K. Hugl, K. Kalliola, and J. Laurila, "Spatial reciprocity of uplink and downlink radio channels in FDD systems," in *Proc. COST*, 2002, vol. 273, no. 2, p. 066.

[26] B. K. Chalise, L. Haering, and A. Czylwik, "Robust uplink to downlink spatial covariance matrix transformation for downlink beamforming," in *Proc. IEEE Int. Conf. Commun. (ICC)*, vol. 5, Jun. 2004, pp. 3010–3014.

[27] M. Jordan, X. Gong, and G. Ascheid, "Conversion of the spatio-temporal correlation from uplink to downlink in FDD systems," in *Proc. IEEE Wireless Commun. Netw. Conf.*, Apr. 2009, pp. 1–6.

[28] M. Arnold, S. Dörner, S. Cammerer, S. Yan, J. Hoydis, and S. ten Brink, "Enabling FDD massive MIMO through deep learning-based channel prediction," 2019, *arXiv:1901.03664*. [Online]. Available: http://arxiv.org/abs/1901.03664

[29] N. GonzÃĺlez-Prelcic, A. Ali, V. Va, and R. W. Heath, Jr., "Millimeter-wave communication with out-of-band information," *IEEE Commun. Mag.*, vol. 55, no. 12, pp. 1038–1052, Dec. 2017.

[30] A. Ali, N. González-Prelcic, and R. W. Heath, Jr., "Millimeter wave beam-selection using out-of-band spatial information," *IEEE Trans. Wireless Commun.*, vol. 17, no. 2, pp. 140–146, Nov. 2017.

[31] A. Ali, N. Gonzalez-Prelcic, and R. W. Heath, "Estimating millimeter wave channels using out-of-band measurements," in *Proc. Inf. Theory Appl. Workshop (ITA)*, Jan. 2016, pp. 1–6.

[32] R. Deng, Z. Jiang, S. Zhou, S. Cui, and Z. Niu, "A two-step learning and interpolation method for location-based channel database construction," in *Proc. IEEE Global Commun. Conf. (GLOBECOM)*, Dec. 2018, pp. 1–6.

[33] P. Dong, H. Zhang, and G. Y. Li, "Machine learning prediction based CSI acquisition for FDD massive MIMO downlink," in *Proc. IEEE Global Commun. Conf. (GLOBECOM)*, Dec. 2018, pp. 1–6.

[34] M. Najla, D. Gesbert, Z. Becvar, and P. Mach, "Machine learning for power control in D2D communication based on cellular channel gains," in *Proc. IEEE Globecom Workshops (GC Wkshps)*, Dec. 2019, pp. 1–6.

[35] X. Li, R. Shankaran, M. A. Orgun, G. Fang, and Y. Xu, "Resource allocation for underlay D2D communication with proportional fairness," *IEEE Trans. Veh. Technol.*, vol. 67, no. 7, pp. 6244–6258, Jul. 2018.

[36] S. Lin, L. Fu, K. Li, and Y. Li, "Sum-rate optimization for device-to-device communications over Rayleigh fading channel," in *Proc. IEEE 85th Veh. Technol. Conf. (VTC Spring)*, Jun. 2017, pp. 1–6.

[37] Z. Chu, W. Hao, P. Xiao, F. Zhou, and R. Q. Hu, "Low-latency driven energy efficiency for D2D communications," in *Proc. ICC-IEEE Int. Conf. Commun. (ICC)*, May 2019, pp. 1–6.

[38] D. Astely, E. Dahlman, A. Furuskär, Y. Jading, M. Lindström, and S. Parkvall, "LTE: The evolution of mobile broadband," *IEEE Commun. Mag.*, vol. 47, no. 4, pp. 44–51, Apr. 2009.

[39] *Evolved Universal Terrestrial Radio Access (E-UTRA); Physical channels and modulation, V13.5.0, Release 13*, document 3GPP TS 36.211, 2017.

[40] P. Mach and Z. Becvar, "Mobile edge computing: A survey on architecture and computation offloading," *IEEE Commun. Surveys Tuts.*, vol. 19, no. 3, pp. 1628–1656, 3rd Quart., 2017.

[41] D. M. Hawkins, "The problem of overfitting," *J. Chem. Inf. Comput. Sci.*, vol. 44, no. 1, pp. 1–12, Jan. 2004.

[42] D. W. Marquardt, "An algorithm for least-squares estimation of nonlinear parameters," *J. Soc. Ind. Appl. Math.*, vol. 11, no. 2, pp. 431–441, Jun. 1963.

[43] M. T. Hagan and M. B. Menhaj, "Training feedforward networks with the Marquardt algorithm," *IEEE Trans. Neural Netw.*, vol. 5, no. 6, pp. 989–993, Nov. 1994.

[44] L. Melki, S. Najeh, and H. Besbes, "Interference management scheme for network-assisted multi-hop D2D communications," in *Proc. IEEE PIMRC*, Sep. 2016, pp. 1–5.

[45] T. D. Hoang, L. B. Le, and T. Le-Ngoc, "Energy-efficient resource allocation for D2D communications in cellular networks," *IEEE Trans. Veh. Technol.*, vol. 65, no. 9, pp. 6972–6986, Sep. 2016.

[46] P. Kyösti *et al.*, *WINNER II Channel Models*, document IST-4-027756 WINNER II D1.1.2 V1.2, 2007.

[47] *Study on LTE Device to Device Proximity Services; Radio Aspects, V12.0.1, Release 12*, document 3GPP TR 36.843, 2014.

Mehyar Najla (Student Member, IEEE) is currently pursuing the Ph.D. degree with the Department of Telecommunication Engineering, Czech Technical University in Prague, Czech Republic, with a topic Device-to-Device Communication Using Radio Frequency and Visible Light Communication Bands.

In 2016, he joined the 5Gmobile Research Laboratory, Czech Technical University in Prague, with a focus on research related to future mobile networks. He was/is involved in several national research projects focused on the combination of radio frequency and visible light communication for device-to-device communication, machine learning for wireless networks, and mobile networks with flying base stations. In 2019, he was on an internship with EURECOM, France. He has coauthored six conference papers and four journal articles. His research interests include radio resource management in mobile networks, device-to-device communication, hybrid radio frequency and visible light communication systems, machine learning for prediction and optimization in mobile networks, game theoretic techniques for resource allocation in wireless networks, and optimization of mobile networks with flying base stations.

Zdenek Becvar (Senior Member, IEEE) received the M.Sc. and Ph.D. degrees in telecommunication engineering from Czech Technical University (CTU) in Prague, Czech Republic, in 2005 and 2010, respectively. From 2006 to 2007, he joined the Sitronics Research and Development Center, Prague, with a focus on speech quality in VoIP. Furthermore, he was involved in research activities of Vodafone Research and Development Center, CTU, in 2009. He was on internships at Budapest Polytechnic, Hungary, in 2007, CEA-Leti, France, in 2013, and EURECOM, France, in 2016 and 2019. From 2013 to 2017, he was a Representative of CTU in ETSI and 3GPP standardization organizations. In 2015, he founded the 5Gmobile Research Laboratory, CTU, with a focus on research toward 5G and beyond mobile networks. He is currently an Associate Professor with the Department of Telecommunication Engineering, CTU. He has published four book chapters and more than 70 conference papers or journal articles. He works on the development of solutions for future mobile networks with a special focus on optimization of mobility and radio resource management, energy efficiency, device-to-device communication, edge computing, C-RAN, self-optimization, and architecture of radio access network.

Pavel Mach (Member, IEEE) received the M.Sc. and Ph.D. degrees in telecommunication engineering from Czech Technical University (CTU) in Prague, Czech Republic, in 2006 and 2010, respectively.

From 2006 to 2007, he joined the Sitronics Research and Development Center, Prague, with a focus on emerging mobile technologies, and he was involved in research activities of Vodafone Research and Development Center, CTU, from 2005 to 2008. He is currently a Senior Researcher with the 5G Mobile Laboratory founded in 2015 at CTU, focusing on 5G and beyond mobile networks. He was involved in several European projects, such as FP6 FIREWORKS, FP7 ROCKET, FP7 FREEDOM, and FP7 TROPIC. He was/is a Principal Investigator in national research projects focused on the allocation of radio resources to cognitive small cells and combination of device-to-device communication with visible light communication. He has published three book chapters and more than 60 conference papers or journal articles and holds one patent. He was on internship with EURECOM, France, in 2019. His current research interests include radio resource management for device-to-device communication, new techniques for dynamic functional split for C-RAN-based network architectures, positioning of flying mobile base stations, and mobile edge computing.

David Gesbert (Fellow, IEEE) received the Ph.D. degree from the Ecole Nationale Superieure des Telecommunications, France, in 1997. From 1997 to 1999, he has been with the Information Systems Laboratory, Stanford University. He was then a Founding Engineer of Iospan Wireless Inc., a Stanford spin-off pioneering MIMO-OFDM (now Intel). Before joining EURECOM in 2004, he has been with the Department of Informatics, University of Oslo, as an Adjunct Professor. He is currently a Professor and the Head of the Communication Systems Department, EURECOM. He has published about 300 articles and holds 25 patents, some of them received the 2019 ICC Best Paper Award, the 2015 IEEE Best Tutorial Paper Award (Communications Society), the 2012 SPS *Signal Processing Magazine* Best Paper Award, the 2004 IEEE Best Tutorial Paper Award (Communications Society), the 2005 Young Author Best Paper Award for Signal Processing Society journals, and paper awards at conferences 2011 IEEE SPAWC and 2004 ACM MSWiM. Since 2015, he has been holding the ERC Advanced grant "PERFUME" on the topic of smart device communications in future wireless networks. He is a Board Member of the OpenAirInterface (OAI) Software Alliance. Since 2019, he has been Head of the Huawei-funded Chair on Advanced Wireless Systems Towards 6G Networks. He sits on the Advisory Board of the HUAWEI European Research Institute. In 2020, he was awarded funding by the French Interdisciplinary Institute on Artificial Intelligence for a Chair in the area of AI for the future IoT. He has been the Technical Program Co-Chair for ICC2017. He was named as a Thomson-Reuters Highly Cited Researcher in Computer Science.